

TOTAL CROSS SECTION OF THE PROCESS $e^+e^- \rightarrow \pi^+\pi^-\pi^+\pi^-$ IN THE C.M.ENERGY RANGE 980–1380 MEV

R.R. Akhmetshin^a, V.M. Aulchenko^{a,c}, V.Sh. Banzarov^a,
A. Baratt^d, L.M. Barkov^{a,c}, N.S. Bashtovoy^a, A.E. Bondar^{a,c},
D.V. Bondarev^a, A.V. Bragin^a, S.I. Eidelman^{a,c},
D.A. Epifanov^a, G.V. Fedotovitch^{a,c}, N.I. Gabyshev^a,
D.A. Gorbachev^a, A.A. Grebeniuk^a, D.N. Grigoriev^{a,c},
F.V. Ignatov^a, S.V. Karpov^a, V.F. Kazanin^{a,c}, B.I. Khazin^{a,c},
I.A. Koop^{a,c}, P.P. Krovkovny^{a,c}, A.S. Kuzmin^{a,c},
I.B. Logashenko^{a,b}, P.A. Lukin^a, A.P. Lysenko^a,
K.Yu. Mikhailov^a, A.I. Milstein^{a,c}, I.N. Nesterenko^{a,c},
V.S. Okhapkin^a, A.V. Otboev^a, E.A. Perevedentsev^{a,c},
A.A. Polunin^a, A.S. Popov^a, S.I. Redin^a, N.I. Root^a,
A.A. Ruban^a, N.M. Ryskulov^a, A.G. Shamov^a,
Yu.M. Shatunov^a, B.A. Shwartz^{a,c}, A.L. Sibidanov^a,
V.A. Sidorov^a, A.N. Skrinsky^a, I.G. Snopkov^a, E.P. Solodov^{a,c},
J.A. Thompson^d, A.A. Valishev^a, Yu.V. Yudin^a,
A.S. Zaitsev^{a,c}, S.G. Zverev^a

^a*Budker Institute of Nuclear Physics, Novosibirsk, 630090, Russia*

^b*Boston University, Boston, MA 02215, USA*

^c*Novosibirsk State University, Novosibirsk, 630090, Russia*

^d*University of Pittsburgh, Pittsburgh, PA 15260, USA*

Abstract

The $e^+e^- \rightarrow \pi^+\pi^-\pi^+\pi^-$ cross section has been measured using 5.8 pb^{-1} of integrated luminosity collected with the CMD-2 detector at the VEPP-2M collider. Analysis of the data with a refined efficiency determination and use of both three- and four-track events allowed doubling of a data sample and reduction of systematic errors to 5-7%.

Introduction

Production of four pions in e^+e^- annihilation is the dominant process contributing to the total hadronic cross section in the c.m. energy range between 1000 and 2000 MeV. Precise measurements of the cross sections of the reactions $e^+e^- \rightarrow 2\pi^+2\pi^-$, $\pi^+\pi^-2\pi^0$ will improve the accuracy of the calculation of the hadronic contribution to the muon anomalous magnetic moment [1, 2] and provide an important input to tests of the relation between the cross sections of the process $e^+e^- \rightarrow 4\pi$ and the differential rate of the $\tau^\pm \rightarrow (4\pi)^\pm\nu_\tau$ decay following from the conservation of the vector current and isospin symmetry [2, 3]. As one of the possible decay modes of the isovector vector states, a four-pion final state and various mechanisms of its production can provide information on the properties of the ρ excitations as well as shed light on the problem of existence of light exotic states (hybrids) between 1000 and 2000 MeV [4, 5].

Although the process $e^+e^- \rightarrow 2\pi^+2\pi^-$ has been extensively studied before in the c.m. energy range 1000–1400 MeV by various groups at the VEPP-2M collider in Novosibirsk [6, 7, 8, 9, 10], the scatter of the obtained results as well as their systematic uncertainties are rather big. In the previous analysis of this process at CMD-2, which was focused on its dynamics, we reported on the first observation of the $a_1(1260)\pi$ dominance [9]. Later this result was confirmed by the CLEO [11] and SND [10] groups. In this paper we present a new analysis of the same data sample based on 5.8 pb^{-1} of integrated luminosity collected at CMD-2 at 36 energy points in the 980–1380 MeV range with a 10 MeV step. A new reconstruction algorithm combined with refined detector calibrations and an update of the integrated luminosity [12] as well as use of both three- and four-track events for the cross section determination allowed a new measurement of the cross section with smaller statistical and systematic uncertainties. The values of the cross section obtained in this work supersede our previous results in [9].

The general purpose detector CMD-2 has been described in detail elsewhere [13]. Its tracking system consists of a cylindrical drift chamber (DC) and double-layer multiwire proportional Z-chamber, both also used for a trigger, and both inside a thin ($0.38 X_0$) superconducting solenoid with a field of 1 T. The barrel CsI calorimeter with a thickness of $8.1 X_0$ is placed outside the solenoid and the end-cap BGO calorimeter with a thickness of $13.4 X_0$ is placed inside the solenoid. The luminosity is measured using events of Bhabha scattering at large angles [14].

Selection of $e^+e^- \rightarrow \pi^+\pi^-\pi^+\pi^-$ Events

Candidates for the process under study were selected from a data sample containing three and more charged tracks reconstructed in the DC and possessing the following properties:

- A track contains more than six points in the R- ϕ plane.
- A track momentum does not exceed a beam momentum by more than 10%.
- A minimum distance from the track to the beam axis in the R- ϕ plane is less than 0.5 cm.
- A minimum distance from the track to the center of the interaction region along Z is less than 10 cm.
- A track has a polar angle θ big enough to cross half of the DC radius and produce enough hits of the DC wires for a good track reconstruction.

Events with three and four tracks satisfying the above requirements were considered as candidates for the $e^+e^- \rightarrow \pi^+\pi^-\pi^+\pi^-$ process. About 26200 four-track events and 22800 three-track events were selected. The number of events with five or more selected tracks was found to be negligible.

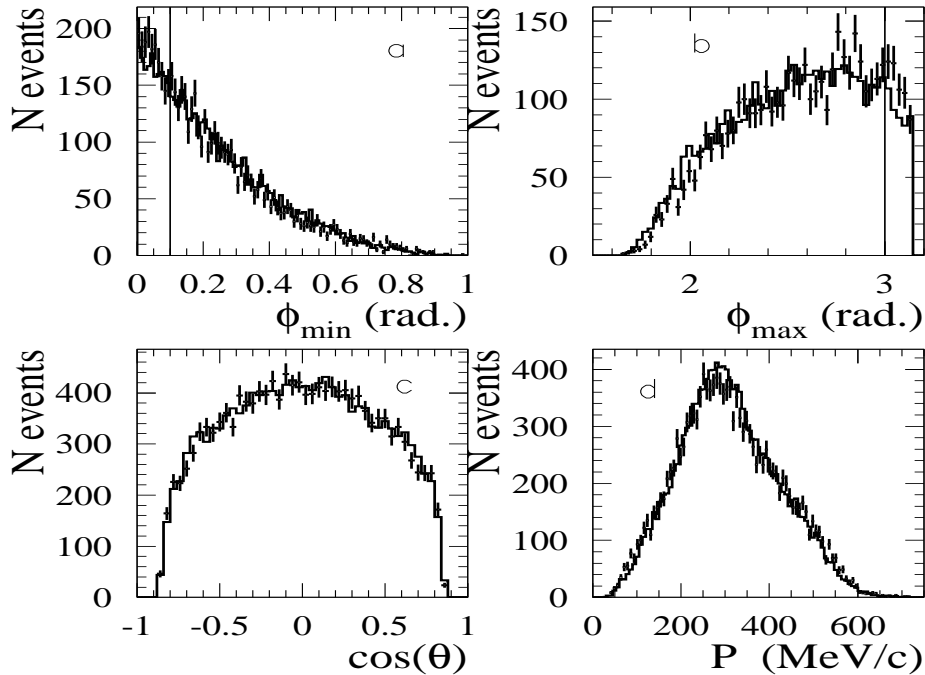


Fig. 1. Distributions for four-track experimental events (points with errors) and simulation (histograms) at $2E_{\text{beam}}=1380$ MeV: (a) Minimum angle between two tracks in the R- ϕ plane; (b) Maximum angle between two tracks in the R- ϕ plane; (c) Cosine of the track polar angle; (d) Track momentum. The lines show applied cuts.

Reconstructed momenta and angles of the tracks for four-track events were used for further selection. Figure 1 presents various distributions for selected events at $2E_{\text{beam}}=1380$ MeV.

The following cuts are additionally applied to further suppress background events. A requirement for a minimum angle between two tracks in the R- ϕ plane to be greater than 0.1 radian removes background events from the processes $e^+e^- \rightarrow \pi^+\pi^-\pi^0(\pi^0)$ with photon conversion to an e^+e^- pair, see Fig. 1(a). A requirement for a maximum angle between two tracks in the R- ϕ plane to be less than 3.0 radian suppresses background from the K^+K^- pair production (kaons have a high probability to decay inside the DC and produce additional tracks) and cosmic showers, see Fig. 1(b). Figures 1(c),(d) present the $\cos(\theta)$ and momentum distributions for detected tracks after applying cuts on relative angles. Results of the Monte Carlo simulation (MC) presented by open histograms well describe the kinematical parameters in Figs. 1(a)-(d).

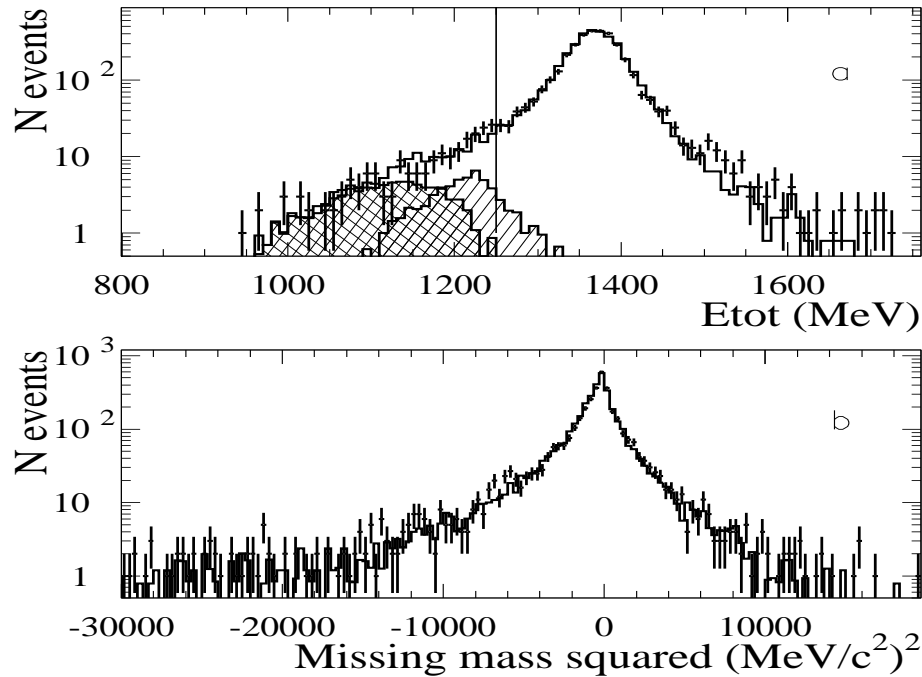


Fig. 2. Distributions for four-track experimental events (points with errors) and simulation (open histograms) at $2E_{\text{beam}} = 1380$ MeV: (a) The total energy of four pions. The hatched and cross-hatched histograms show the contributions from five-pion production ($\omega\pi^+\pi^-$ and $\eta\pi^+\pi^-$, respectively). The line shows an applied cut; (b) Missing mass squared for four pions.

Figure 2(a) presents the total energy distribution for events with four tracks after the above selections at $2E_{\text{beam}} = 1380$ MeV. The only remaining source of background is the production of the five-pion final state ($e^+e^- \rightarrow \omega\pi^+\pi^-$ and $e^+e^- \rightarrow \eta\pi^+\pi^-$

with ω and η decays to $\pi^+\pi^-\pi^0$), which results in a lower total energy because of a missing π^0 . The contributions of these channels are shown in Fig. 2(a) by the hatched and cross-hatched histograms, respectively, and the histograms were obtained from simulation and the values of the corresponding cross sections measured at CMD-2 [15]. The applied cut $E_{\text{tot}} > 2E_{\text{beam}} - 130$ MeV shown by the vertical line almost completely removes these events. The missing mass squared distribution after this cut is shown in Fig. 2(b) in comparison with simulation. For four-track events the remaining background is estimated to be less than 1%.

To increase the data sample and improve a systematic uncertainty related to the efficiency determination, a sample of events with three selected tracks was additionally used to determine the number of four-pion events with one missing track. A track can be lost for one of the following reasons: it flies at small polar angles outside the efficient DC region, decays in flight, because of incorrect reconstruction, due to nuclear interactions, by overlapping with another track. From energy-momentum conservation the direction and momentum of a missing track can be calculated assuming a four-pion final state. The reconstructed momentum vectors were used to apply the additional requirements on the angles between two tracks in the R - ϕ plane described above.

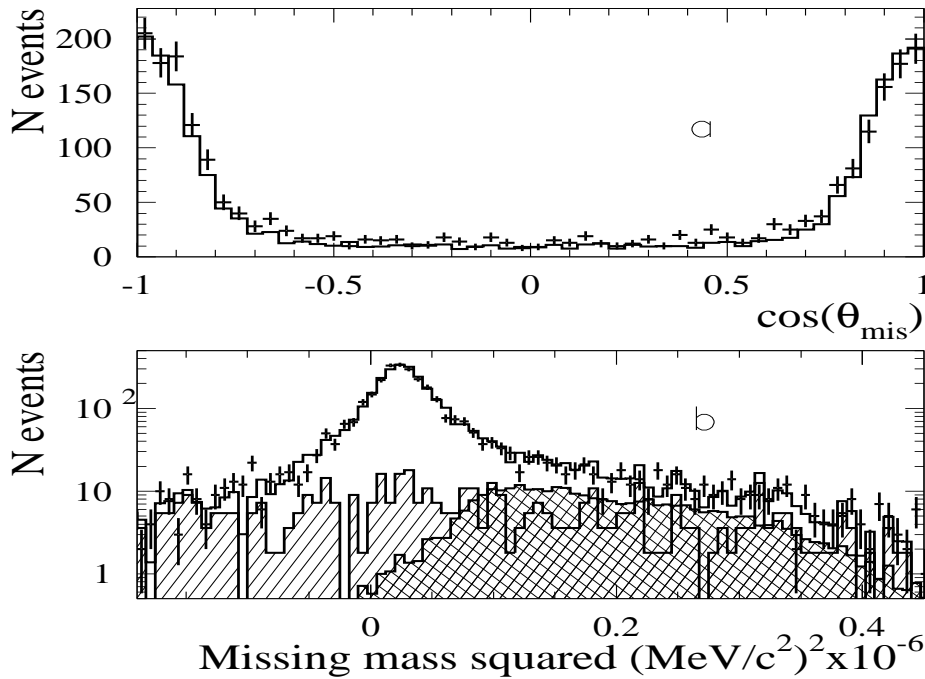


Fig. 3. Distributions for three-track experimental events (points with errors): (a) Cosine of a polar angle for a missing pion, the open histogram shows results of the simulation; (b) Missing mass squared distribution for the three-track sample. The open histogram shows results of the simulation. The hatched histogram shows a contribution from beam-gas background. The cross-hatched histogram shows a contribution from five-pion events.

Figure 3(a) shows the $\cos(\theta)$ distribution for a missing pion after the cuts on the angles between two tracks. It can be seen that most of the three-track events have a fourth track flying at small angles with respect to the beam axis and not detected by the DC. In some cases the missing track is inside the DC acceptance but does not meet the selection criteria.

The three-track event sample has higher background than the four-track one, but events corresponding to the four-pion final state could be separated by requiring that a missing particle have the charged pion mass. The distribution of missing mass squared for three-track events is shown in Fig. 3(b) and exhibits a clear signal at the pion mass that can be attributed to four-pion events. The background in this sample comes mostly from five-pion events and beam-gas interactions. The latter source results in a relatively flat distribution over missing mass and can be estimated from the events in the $7.0 < |Z| < 10.0$ cm region (the longitudinal size of the collision region has r.m.s. about 2 cm). This contribution is shown by the hatched histogram in Fig. 3(b). The contribution from five-pion events estimated from the MC simulation is shown by the cross-hatched histogram in Fig. 3(b).

To obtain the number of four-pion events from a three-track sample, the distribution shown in Fig. 3(b) was fit with a sum of functions describing a pion peak and background. The pion peak line shape was taken from simulation of the four-pion process and had a Gaussian shape with a small radiative tail. All parameters of this function were fixed except for the number of events. A second order polynomial with all free parameters was used for background. As a result of the fit, the number of four-pion events in the three-track sample was determined.

To check stability of the background subtraction procedure, the number of four-pion events was independently estimated by statistical subtraction of background shown in Fig. 3(b). This procedure gives results consistent with those from the fit, but has slightly higher errors in the number of four-pion events. The 2% variation in the number of events between the two subtraction procedures was taken as an estimate of a systematic error.

About 20550 four-track and 17180 three-track events survive at this stage of selection. The number of four- and three-track events determined at each energy is listed in Table 1.

Table 1

Luminosity, number of events, detection efficiency, rad. correction, cross section and vacuum polarization correction

$2E_{\text{beam}}$, MeV	L, nb^{-1}	N_{4tr}	N_{3tr}	ϵ_{MC}	$1 + \delta$	σ , nb	$ 1 - \Pi(2E_{\text{beam}}) ^2$
980.0	59.00	7	7.32 ± 4.08	0.426	0.880	0.65 ± 0.22	0.9751
1040.0	72.76	25	32.00 ± 8.05	0.442	0.881	2.01 ± 0.33	0.9583
1050.0	116.03	44	47.65 ± 7.99	0.444	0.882	2.02 ± 0.23	0.9622
1060.0	75.71	40	35.15 ± 7.03	0.447	0.882	2.52 ± 0.32	0.9643
1070.0	80.63	43	36.16 ± 7.04	0.449	0.882	2.48 ± 0.30	0.9657
1080.0	59.00	37	32.77 ± 7.03	0.452	0.883	2.96 ± 0.40	0.9666
1090.0	83.58	58	60.81 ± 8.80	0.454	0.883	3.55 ± 0.35	0.9674
1100.0	57.03	50	43.56 ± 7.51	0.456	0.883	4.07 ± 0.45	0.9679
1110.0	82.60	62	69.30 ± 9.44	0.458	0.885	3.92 ± 0.37	0.9684
1120.0	58.01	37	54.00 ± 9.70	0.460	0.885	3.85 ± 0.48	0.9688
1130.0	96.36	101	90.82 ± 10.70	0.462	0.886	4.86 ± 0.37	0.9692
1140.0	96.36	129	110.85 ± 11.57	0.464	0.885	6.05 ± 0.41	0.9695
1150.0	52.11	66	52.73 ± 8.29	0.466	0.887	5.51 ± 0.54	0.9697
1160.0	111.11	155	135.56 ± 12.64	0.468	0.886	6.30 ± 0.38	0.9700
1170.0	90.46	136	130.49 ± 17.91	0.470	0.888	7.05 ± 0.57	0.9702
1180.0	113.08	204	177.41 ± 14.87	0.472	0.889	8.04 ± 0.43	0.9704
1190.0	128.81	256	246.67 ± 18.12	0.474	0.889	9.27 ± 0.45	0.9706
1200.0	183.87	417	339.41 ± 19.96	0.475	0.890	9.73 ± 0.37	0.9708
1210.0	120.94	295	215.23 ± 16.56	0.477	0.892	9.92 ± 0.46	0.9711
1220.0	111.11	323	229.16 ± 16.78	0.479	0.892	11.65 ± 0.52	0.9712
1230.0	140.61	422	332.33 ± 19.81	0.480	0.891	12.54 ± 0.47	0.9714
1240.0	141.59	460	314.80 ± 19.51	0.481	0.893	12.73 ± 0.48	0.9716
1250.0	208.46	627	579.42 ± 31.68	0.483	0.894	13.41 ± 0.45	0.9717
1260.0	176.99	677	492.77 ± 23.78	0.484	0.894	15.26 ± 0.46	0.9719
1270.0	242.87	912	751.12 ± 29.63	0.485	0.896	15.75 ± 0.40	0.9721
1280.0	219.27	859	684.76 ± 29.13	0.487	0.896	16.14 ± 0.43	0.9723
1290.0	285.15	1067	1011.61 ± 41.13	0.488	0.898	16.64 ± 0.42	0.9724
1300.0	279.09	1256	949.54 ± 33.03	0.489	0.898	17.99 ± 0.40	0.9726
1310.0	231.07	1055	829.30 ± 31.40	0.490	0.899	18.50 ± 0.44	0.9728
1320.0	191.74	893	779.53 ± 30.26	0.491	0.901	19.72 ± 0.50	0.9730
1330.0	320.66	1377	1337.15 ± 43.74	0.492	0.902	19.07 ± 0.40	0.9732
1340.0	204.52	1170	754.22 ± 30.03	0.493	0.904	21.12 ± 0.50	0.9734
1350.0	229.11	1085	1101.86 ± 41.34	0.494	0.904	21.37 ± 0.52	0.9737
1360.0	313.67	1615	1499.79 ± 45.99	0.495	0.906	22.16 ± 0.43	0.9739
1370.0	186.82	1023	935.66 ± 36.41	0.495	0.907	23.35 ± 0.58	0.9742
1380.0	575.22	3568	2617.01 ± 68.22	0.496	0.909	23.86 ± 0.35	0.9746

Detection efficiency from simulation

The detailed study of the process dynamics performed in [9] showed that the $a_1(1260)\pi$ intermediate mechanism dominates the final state with four charged pions. Various observed distributions were investigated in that analysis to search for a possible admixture of some other mechanisms like $\rho f_0(600)$, $a_2(1320)\pi$, $\pi(1300)\pi$ etc. It was shown that the $a_1(1260)\pi$ by itself can account for the observed spectra although a small admixture of

other mechanisms can not be excluded. The highest upper limit for a possible admixture, equal to 15%, was obtained for the $\pi(1300)\pi$ model. Therefore, for Monte Carlo simulation and studies of the detection efficiency (acceptance) we used the $a_1(1260)\pi$ and $\pi(1300)\pi$ models described in [9]. The two-pion invariant mass experimental spectra shown in Fig. 4 together with those from the simulation within the $a_1(1260)\pi$ model at $2E_{\text{beam}} = 1380$ MeV qualitatively agree with each other. The model with a 15% admixture of the $\pi(1300)\pi$ mechanism gives mass distributions indistinguishable from those for the $a_1(1260)\pi$ model.

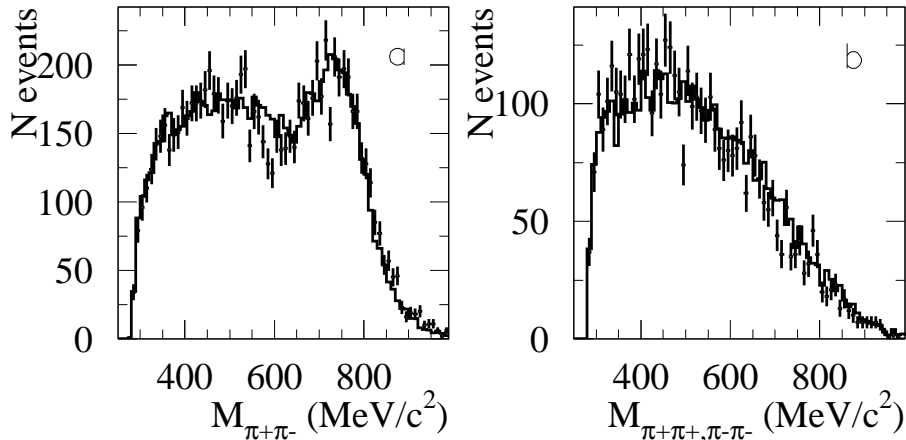


Fig. 4. Di-pion mass distributions for experimental events (points with errors) and simulation (histograms): (a) $\pi^+\pi^-$ mass spectrum; (b) $\pi^\pm\pi^\pm$ mass spectrum

The detection efficiency was determined from MC simulation using both four- and three-track events. It should be pointed out that in this case possible data-MC inconsistencies in the description of the DC inefficiency and (partly) in the model-dependent angular distributions are compensated, because in case of an undetected track an event migrates from the four- to the three-track sample. MC simulation was performed at nine energy points from 980 to 1380 MeV and 30000 events were generated at each of these points. The detection efficiency thus obtained monotonously grows from 42.6% to 49.6% in the energy range studied. Its values at each energy point shown in Table 1 were calculated using the polynomial approximation of the detection efficiency determined at the nine points mentioned above. Its statistical error is less than 1%.

Cross Section Calculation

At each energy the cross section was calculated as

$$\sigma = \frac{N_{4\text{tr}} + N_{3\text{tr}}}{L \cdot \epsilon \cdot (1 + \delta)},$$

where L is the integrated luminosity for this energy point, ϵ is the detection efficiency obtained from the MC simulation and $(1 + \delta)$ is the radiative correction calculated according to [16]. The charged trigger efficiency was studied in Ref. [17] where it was shown that for two tracks the trigger efficiency was $(98.3 \pm 0.9 \pm 0.5)\%$. Since only one charged track is sufficient for a trigger, we assume that for multitrack events considered in this analysis the trigger efficiency is close to 100%.

The integrated luminosity, the number of four and three-track events, detection efficiency, radiative correction and obtained cross section for each energy point are listed in Table 1. Table 1 also contains a so called vacuum polarization correction factor $|1 - \Pi(2E_{\text{beam}})|^2$, where $\Pi(2E_{\text{beam}})$ is the polarization operator. Multiplying it by the “dressed” cross section presented in Table 1, one obtains the “bare” cross section to be used in dispersion integral calculations (see, e.g., the discussion in Ref. [12]).

Systematic errors

The following sources of systematic uncertainties were considered.

- The model dependence of the acceptance is determined by the angular distribution, which is specific for each particular model. Therefore, we compared results of the cross section calculation for different $\cos(\theta)$ cuts in two models of the final state production: the dominant $a_1(1260)\pi$ mechanism and $\pi(1300)\pi$, which admixture at the 15% level, as discussed above, was not excluded by the analysis in [9]. The resulting systematic uncertainty caused by model and angular cut dependence is estimated as 3%.
- A systematic error because of the selection criteria other than the angular cuts was studied by varying the cuts described previously and doesn't exceed 2%.
- The uncertainty in the determination of the integrated luminosity comes from the selection criteria of Bhabha events, radiative corrections and calibrations of DC and CsI and does not exceed 2% [14].
- The contribution of the uncertainty of the charged trigger inefficiency studied with $\phi \rightarrow K_S^0 K_L^0$ events [17] appears to be much less than 1% and can be neglected.

- A possible uncertainty in the beam energy was studied using the momentum distribution of Bhabha events and total energy of four-pion events. The uncertainty at the level of 10^{-3} was not excluded and because of the relatively fast cross section variation it can result in a 1% change of the cross section.
- A radiative correction uncertainty was estimated as about 1% mainly due to the uncertainty in the maximum allowed energy of the emitted photon at the integration of the formulae from [16] as well as the accuracy of these formulae.
- The uncertainty because of background subtraction for four-track (three-track) events is estimated as 1% (2%) above 1100 MeV growing to 5% below 1100 MeV for both types of events. At low energy the cross sections of the processes $e^+e^- \rightarrow \pi^+\pi^-\pi^0$ and $e^+e^- \rightarrow \pi^+\pi^-2\pi^0$ dominating the background are considerably higher than that of the process under study.

The above systematic uncertainties summed in quadrature give an overall systematic error of about 5% above 1100 MeV and about 7% below 1100 MeV. This uncertainty is common (energy-independent) for most of the energy range studied. Some energy-dependent contribution to the total experimental uncertainty is possible below 1100 MeV, but there the systematic error is much smaller than a statistical one.

Discussion

From Fig. 5 it is clear that the obtained values of the cross section are consistent with the results of the precise measurement performed by the SND group [10]. They are also in good agreement with the other previous experiments in the energy range studied [6, 7, 8]. The three-track events used in this analysis allowed a significant increase of the data sample and improvement of the systematic uncertainties.

The rapid growth of the cross section with energy is apparently due to the $\rho(1450)$ and $\rho(1700)$. The maximum energy of our experiment is insufficient for a quantitative study of these resonances which parameters are currently known with rather bad precision [18]. We hope that future experiments at the VEPP-2000 collider currently under construction in Novosibirsk [19] will allow a detailed investigation of both 4π final states from threshold to 2000 MeV.

Let us estimate the implication of our results for the corresponding contribution to

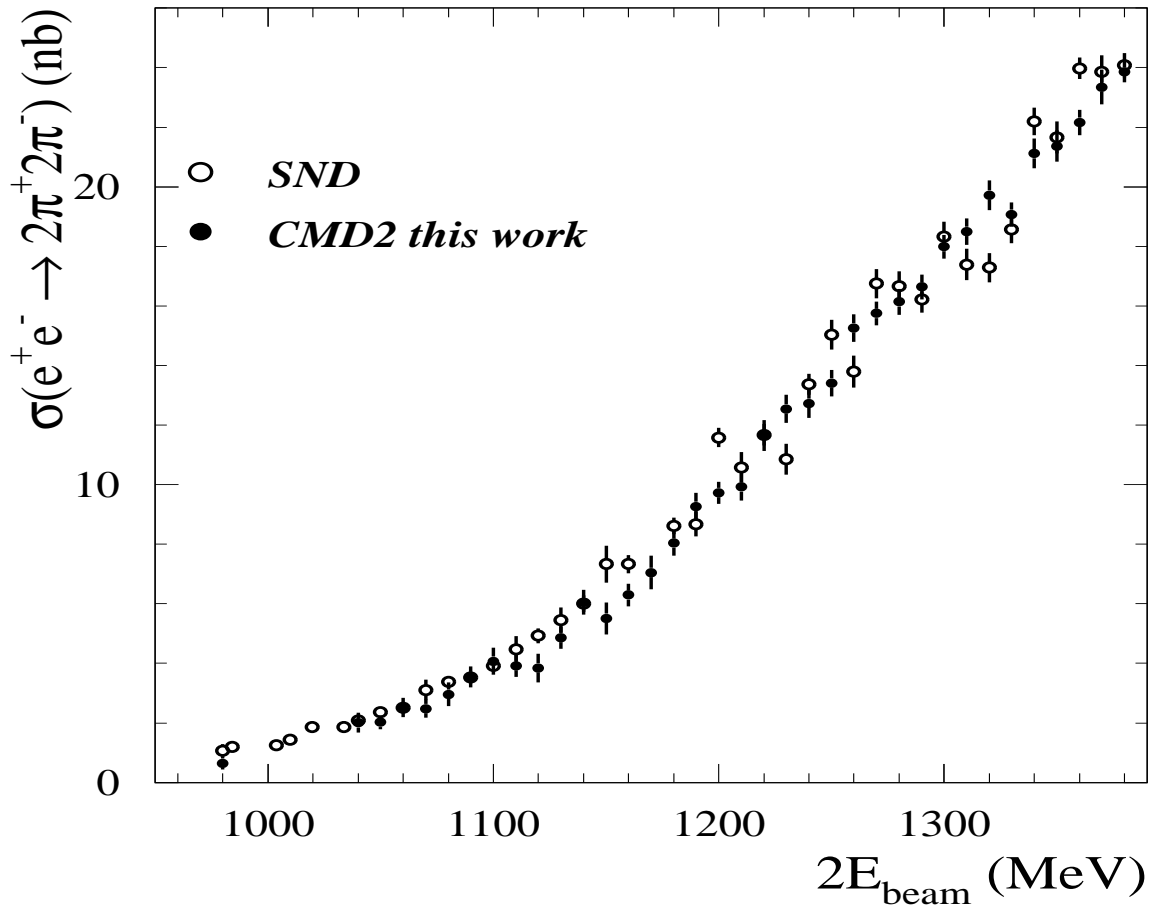


Fig. 5. Cross section of the process $e^+e^- \rightarrow \pi^+\pi^-\pi^+\pi^-$ obtained in two most precise experiments in the 900-1400 MeV energy range. Only statistical errors are shown.

$a_\mu^{\text{had,LO}}$, the leading order hadronic term in the muon anomalous magnetic moment. To this end we calculate its value in the c.m.energy range studied in this work (from 1040 to 1380 MeV) using recent precise data from SND and CMD-2 and compare it to that based on the previous e^+e^- measurements [6, 7, 8] in Table 2.

The first line of the Table (Old data) gives the result based on the data of OLYA, CMD and ND while the second one (New data) is obtained from the recent data of SND and CMD-2, which are in good agreement with each other: $(4.36 \pm 0.31) \cdot 10^{-10}$ (SND) vs. $(4.24 \pm 0.20) \cdot 10^{-10}$ (CMD-2). The third line (Old + New) presents the weighted average of these two estimates. For convenience, we list separately statistical and systematic uncertainties in the second column while the third one gives the total error obtained by adding them in quadrature. One can see that the estimate based on the new data is in good agreement with that coming from the old data. Because of the large number of energy points in all the measurements at VEPP-2M, an overall statistical error is much smaller than a corresponding systematic uncertainty for both old and new data. The statistical precision of the new measurements with SND and CMD-2 is three times

Table 2

Contributions of the $2\pi^+2\pi^-$ channel to $(g_\mu - 2)/2$		
Data	$a_\mu^{\text{had,LO}}, 10^{-10}$	Total error, 10^{-10}
Old	$4.40 \pm 0.06 \pm 0.31$	0.31
New	$4.28 \pm 0.02 \pm 0.17$	0.17
Old + New	$4.31 \pm 0.02 \pm 0.15$	0.15

higher than before and the total error is almost a factor of two smaller than earlier. The combined value based on both old and new data is dominated by the new measurements and provides a significant improvement of the accuracy in the $2\pi^+2\pi^-$ contribution to $a_\mu^{\text{had,LO}}$. Although the relative contribution to $a_\mu^{\text{had,LO}}$ of the considered channel and the energy range from 980 to 1380 MeV is small, in combination with the $\pi^+\pi^-2\pi^0$ final state the 4π production is responsible for about 57% of the contribution to $a_\mu^{\text{had,LO}}$ from the hadronic continuum below 2000 MeV, i.e. production of hadrons not from the ρ , ω and ϕ . Therefore, significant improvement of the precision of its cross section is of extreme importance for the interpretation of the current and future measurements of the muon anomalous magnetic moment [20].

Conclusion

The total cross section of the process $e^+e^- \rightarrow \pi^+\pi^-\pi^+\pi^-$ has been measured using 5.8 pb⁻¹ of integrated luminosity collected with the CMD-2 detector at the VEPP-2M e^+e^- collider. The new refined analysis based on the extraction of the detector efficiency from three- and four-track event samples results in a factor of two larger data sample and allows reduction of systematic errors. The observed production mechanism is consistent with the $a_1(1260)\pi$ intermediate state. The values of the obtained cross section are in good agreement with all other experiments in the energy range studied and supersede our previous results based on the same data sample [9].

Acknowledgments

The authors are grateful to V.P. Druzhinin and Z.K. Silagadze for useful discussions. This work is supported in part by grants DOE DEFG0291ER40646, NSF PHY-9722600, NSF PHY-0100468, PST.CLG.980342, RFBR-02-02-16126-a, RFBR-03-02-10843 and RFBR-04-02-16223-a.

REFERENCES

1. T. Kinoshita, B. Nižić and Y. Okamoto, Phys. Rev. **D31** (1985) 2108.
2. M. Davier *et al.*, Eur. Phys. J. **C27** (2003) 497.
3. A.E. Bondar *et al.*, Phys. Lett. **B466** (1999) 403.
4. T. Barnes *et al.*, Phys. Rev. **D55** (1997) 4157.
5. A. Donnachie and Yu.S. Kalashnikova, Phys. Rev. **D60** (1999) 114001.
6. L.M. Kurdadze *et al.*, JETP Lett. **47** (1988) 512.
7. L.M. Barkov *et al.*, Sov. J. Nucl. Phys. **47** (1988) 248.
8. S.I. Dolinsky *et al.*, Physics Reports **99** (1991) 202.
9. R.R. Akhmetshin *et al.*, Preprint BudkerINP 98-83, Novosibirsk 1998; Phys. Lett. **B466** (1999) 392.
10. M.N. Achasov *et al.*, JETP **96** (2003) 789.
11. K.W. Edwards *et al.*, Phys. Rev. **D61** (2000) 072003.
12. R.R. Akhmetshin *et al.*, Phys. Lett. **B578** (2004) 285.
13. G.A. Aksenov *et al.*, Preprint BudkerINP 85-118, Novosibirsk, 1985.
E.V. Anashkin *et al.*, ICFA Instrumentation Bulletin **5** (1988) 18.
14. R.R. Akhmetshin *et al.*, Preprint Budker INP 99-11, Novosibirsk, 1999.
15. R.R. Akhmetshin *et al.*, Phys. Lett. **B489** (2000) 125.
16. E.A. Kuraev and V.S. Fadin, Sov. J. Nucl. Phys. **41** (1985) 466.
17. R.R. Akhmetshin *et al.*, Phys. Lett. **B466** (1999) 385.
18. K. Hagiwara *et al.*, Phys. Rev. **D66** (2002) 010001.
19. Yu.M. Shatunov *et al.*, Proc. of EPAC 2000, Vienna, Austria, 2000, p.439.
20. G.W. Bennett *et al.*, hep-ex/0401008.